
Deep kernel machines and fast solvers for deep kernel machines

Laurence Aitchison
University of Bristol, Bristol, UK

Abstract

Deep neural networks (DNNs) with the flexibility to learn good top-layer representations have eclipsed shallow kernel methods without that flexibility. Here, we take inspiration from DNNs to develop the first non-Bayesian deep kernel method, the deep kernel machine. In addition, we develop a solver for the intermediate layer kernels in deep kernel machines that converges in around 10 steps, exploiting matrix solvers initially developed in the control theory literature. These are many times faster the usual gradient descent approach and generalise to arbitrary architectures. While deep kernel machines currently scale poorly in the number of datapoints, we believe that this can be rectified in future work, allowing deep kernel machines to form the basis of a new class of much more efficient deep nonlinear function approximators.

1 Introduction

Deep neural networks (DNNs) have recently eclipsed kernel methods (Smola & Schölkopf, 1998; Shawe-Taylor & Cristianini, 2004; Hofmann et al., 2008), as DNNs give excellent performance on a wide range of previously intractable tasks (e.g. Krizhevsky et al., 2012). The key advantage of a DNN is that depth gives the flexibility to learn a good top-layer representation (Aitchison, 2020). In contrast, in a (shallow) kernel method, the kernel itself can be viewed as the top-layer representation (Aitchison, 2020), and this kernel is highly inflexible — there are usually a few tunable hyperparameters, but nothing that approaches the enormous flexibility of the top-layer representation in a DNN. This raises a critical question:

can we take inspiration from *deep* neural networks to develop a new family of *deep* kernel machine?

There are tantalising hints that the answer is yes. In particular, recent work developed a probabilistic deep kernel method, the deep kernel process (Aitchison et al., 2021; Ober & Aitchison, 2021). In a deep kernel process, there are a number of intermediate layers. Each intermediate layer has a kernel, and a prior and approximate posterior distribution over that kernel. Remarkably, deep kernel process priors generalise Bayesian neural networks (BNNs) and deep Gaussian processes (DGPs), indicating that they parameterise a powerful, flexible function class.

However, most successful neural network and kernel methods are non-Bayesian (Wenzel et al., 2020). As such, here we develop a non-Bayesian deep kernel method, the deep kernel machine. While this might initially seem straightforward, the choice of loss-function is highly non-trivial, as obvious choices such as MAP inference in a deep kernel process fail.

In addition, we show that the simpler form for the deep kernel process loss allows us to optimize the loss using methods inspired by iterative matrix solvers from other fields. The resulting algorithm iteratively solves the continuous algebraic Ricatti equation (CARE), using methods well understood in the control theory literature (e.g. Benner, 1999). Our solver converges in around 10 steps, and is radically new as it does not have a simple interpretation as e.g. a preconditioned gradient method.

As this is only a starting point, there are two key limitations and thus directions for future work. First, at present, the methods developed here will not scale to large datasets, as they are $\mathcal{O}(P^3)$ time and $\mathcal{O}(P^2)$ space, where P is the number of input points. Second, we only do point estimation, and do not approximate a Bayesian posterior. Our work thus opens the tantalising possibility of developing fast, scalable *solvers* using low rank or inducing point approximations which are able to compete with classical neural networks, and of developing new fast-converging Bayesian posterior approximation methods for DKPs.

2 Background

2.1 Continuous algebraic Ricatti equation (CARE)

The CARE is

$$\mathbf{0} = \mathbf{A}^T \mathbf{G} + \mathbf{G} \mathbf{A} - \mathbf{G} \mathbf{U} \mathbf{G} + \mathbf{Q}. \quad (1)$$

The goal is to solve for positive definite \mathbf{G} with positive definite \mathbf{U} and \mathbf{Q} and real \mathbf{A} . This equation can be solved analytically by taking the eigendecomposition of an extended matrix, but rapidly converging iterative solution methods also exist (Kleinman, 1968; Lancaster & Rodman, 1995; Benner, 1999).

2.2 Deep Gaussian processes (DGPs)

A DGP is a multilayer model mapping from inputs, $\mathbf{X} \in \mathbb{R}^{P \times \nu_0}$, to outputs, $\mathbf{Y} \in \mathbb{R}^{P \times \nu_{L+1}}$, with intermediate layer features, $\mathbf{F}_\ell \in \mathbb{R}^{P \times \nu_\ell}$. Here, ν_ℓ is the number of features at layer ℓ , and P is the number of input points. The features are sampled from a Gaussian process (GP) with a kernel that depends on the previous layer features,

$$P(\mathbf{F}_\ell | \mathbf{F}_{\ell-1}) = \prod_{\lambda=1}^{\nu_\ell} \mathcal{N}(\mathbf{f}_\lambda^\ell; \mathbf{0}, \mathbf{K}_{\text{features}}(\mathbf{F}_{\ell-1})) \quad (2)$$

$$P(\mathbf{Y} | \mathbf{F}_{L+1}) = \prod_{\lambda=1}^{\nu_{L+1}} \mathcal{N}(\mathbf{y}_\lambda; \mathbf{f}_\lambda^{L+1}, \sigma^2 \mathbf{I}). \quad (3)$$

where $\mathbf{K}_{\text{features}}$ is a function that converts the previous layer features into the corresponding kernel, corresponding to e.g. typical squared-exponential or Matern kernels. The full feature and target matrices, \mathbf{F}_ℓ and \mathbf{Y} , can be written as a stack of vectors,

$$\begin{aligned} \mathbf{F}_\ell &= (\mathbf{f}_1^\ell \quad \mathbf{f}_2^\ell \quad \cdots \quad \mathbf{f}_{\nu_\ell}^\ell) \\ \mathbf{Y} &= (\mathbf{y}_1 \quad \mathbf{y}_2 \quad \cdots \quad \mathbf{y}_{\nu_{L+1}}). \end{aligned}$$

where each $\mathbf{f}_\lambda^\ell \in \mathbb{R}^P$ or $\mathbf{y}_\lambda \in \mathbb{R}^P$ gives the value of that particular feature or output for all P datapoints.

2.3 Deriving equivalent deep Wishart processes

The deep Wishart process is a specific deep kernel process, with a prior over functions equivalent to the DGP (Aitchison et al., 2021; Ober & Aitchison, 2021). The deep Wishart process dispenses with features, \mathbf{F}_ℓ , and instead works entirely in terms of Gram matrices,

$$\mathbf{G}_\ell = \frac{1}{\nu_\ell} \mathbf{F}_\ell \mathbf{F}_\ell^T = \frac{1}{\nu_\ell} \sum_{\lambda=1}^{\nu_\ell} \mathbf{f}_\lambda^\ell (\mathbf{f}_\lambda^\ell)^T. \quad (4)$$

The first key observation is that the definition of the Gram matrix here, in combination with the prior over \mathbf{F}_ℓ (Eq. 2), mirrors the definition of samples from a Wishart distribution. Thus, we can directly sample

\mathbf{G}_ℓ from a Wishart, rather than needing to first sample underlying features,

$$P(\mathbf{G}_\ell | \mathbf{F}_{\ell-1}) = \mathcal{W}\left(\mathbf{G}_\ell; \frac{1}{\nu_\ell} \mathbf{K}_{\text{features}}(\mathbf{F}_{\ell-1}), \nu_\ell\right). \quad (5)$$

This is the first step towards dispensing with features, and working entirely with Gram matrices. However, computing the kernel still appears to require the features. Remarkably, it turns out that most kernels of interest, including isotropic kernels that depend only on distance, and others such as the arccos kernel (Cho & Saul, 2009) can be written entirely in terms of the Gram matrix, without knowledge of the features. For isotropic kernels,

$$\mathbf{K}_{ij}^\ell = k(R_{ij}^\ell) \quad (6)$$

where the squared distance, R_{ij}^ℓ can be recovered from the Gram matrix,

$$\begin{aligned} R_{ij}^\ell &= \frac{1}{\nu_\ell} \sum_{\lambda=1}^{\nu_\ell} \left((F_{i\lambda}^\ell)^2 - 2F_{i\lambda}^\ell F_{j\lambda}^\ell + (F_{j\lambda}^\ell)^2 \right) \\ &= G_{ii}^\ell - 2G_{ij}^\ell + G_{jj}^\ell. \end{aligned} \quad (7)$$

Therefore, we readily obtain $\mathbf{K}(\cdot)$, a function that takes the previous layer's Gram matrix and returns the kernel,

$$\mathbf{K}_{\text{features}}(\mathbf{F}_{\ell-1}) = \mathbf{K}(\mathbf{G}_{\ell-1}) \quad (8)$$

Now that we can sample the Gram matrix directly from the kernel, and we can compute the kernel directly from the previous layer Gram matrix, we no longer need to represent or work with the underlying features. And this is the key property of a deep kernel process. To formally define the full deep kernel process generatively, we start by taking the initial Gram matrix as,

$$\mathbf{G}_0 = \frac{1}{\nu_0} \mathbf{X} \mathbf{X}^T, \quad (9)$$

Then subsequent Gram matrices can be sampled from a Wishart,

$$P(\mathbf{G}_{\ell \in \{1 \dots L\}} | \mathbf{G}_{\ell-1}) = \mathcal{W}\left(\frac{1}{\nu_\ell} \mathbf{K}(\mathbf{G}_{\ell-1}), \nu_\ell\right), \quad (10)$$

$$P(\mathbf{F}_{L+1} | \mathbf{G}_L) = \prod_{\lambda=1}^{\nu_{L+1}} \mathcal{N}(\mathbf{f}_\lambda^{L+1}; \mathbf{0}, \mathbf{K}(\mathbf{G}_L)), \quad (11)$$

the top-layer features are from a Gaussian process, with kernel given by $\mathbf{K}(\mathbf{G}_L)$ and the outputs are given by Eq. (3), as in the DGP.

3 Methods: deep kernel machines

Deep kernel machines are non-Bayesian variants of deep kernel processes. As such, they also map from inputs, \mathbf{X} , to outputs, \mathbf{Y} , and are parameterised by a series of intermediate layer positive definite Gram matrices, $\mathbf{G}_1, \dots, \mathbf{G}_L$. To find the right intermediate

layer Gram matrices, $\mathbf{G}_1, \dots, \mathbf{G}_L$, we need an objective function, and to design the objective, we take inspiration from the deep kernel process. In particular, in a deep kernel process, we have

$$\mathbb{E} [\mathbf{G}_\ell | \mathbf{G}_{\ell-1}] = \mathbf{K}(\mathbf{G}_{\ell-1}). \quad (12)$$

and indeed, if we send $\nu_\ell \rightarrow \infty$ then we eliminate all flexibility, and the intermediate layer kernels become deterministic,

$$\mathbf{G}_\ell = \mathbf{K}(\mathbf{G}_{\ell-1}). \quad (13)$$

Thus, it seems sensible to use an objective of the form,

$$\mathcal{L} = \log P(\mathbf{Y} | \mathbf{G}_L) + \sum_{\ell=1}^L L(\mathbf{G}_\ell, \mathbf{G}_{\ell-1}) \quad (14)$$

where we take the first term to be,

$$\log P(\mathbf{Y} | \mathbf{G}_L) = \sum_{\lambda=1}^{\nu_{L+1}} \log \mathcal{N}(\mathbf{y}_\lambda; \mathbf{0}, \sigma^2 \mathbf{I} + \mathbf{K}(\mathbf{G}_L)), \quad (15)$$

which encourages good performance on the training data, and where we take $L(\mathbf{G}_\ell; \mathbf{G}_{\ell-1})$ to be a term that encourages \mathbf{G}_ℓ to lie close to $\mathbf{K}(\mathbf{G}_{\ell-1})$; formally, we might require

$$\mathbf{K}(\mathbf{G}_{\ell-1}) = \arg \max_{\mathbf{G}_\ell} [\mathcal{L}(\mathbf{G}_\ell; \mathbf{G}_{\ell-1})]. \quad (16)$$

Now, we consider a number of intuitively reasonable objectives based on the deep kernel process formulation, and ask whether they satisfy this requirement.

Perhaps the most natural approach would be to use $\log P(\mathbf{G}_\ell | \mathbf{G}_{\ell-1})$, which would result in MAP inference in the Gram matrix domain. However, the mode of $\log P(\mathbf{G}_\ell | \mathbf{G}_{\ell-1})$ lies at zero,

$$\mathbf{0} = \arg \max_{\mathbf{G}_\ell} [\log P(\mathbf{G}_\ell | \mathbf{G}_{\ell-1})], \quad (17)$$

so this approach does not satisfy our requirement (Eq. 16). Indeed, its actually much worse than that. The gradient explodes as $\mathbf{G}_\ell \rightarrow \mathbf{0}$, so the loss landscape is highly pathological, and the only reason the maximum is at zero is due to the positive semidefiniteness constraint (Appendix A).

An alternative is to do MAP inference over features, \mathbf{F}_ℓ , rather than Gram matrices,

$$\log P(\mathbf{F}_\ell | \mathbf{F}_{\ell-1}) = T_\ell + D_\ell \quad (18)$$

$$T_\ell = -\frac{\nu_\ell}{2} \text{Tr}(\mathbf{K}^{-1}(\mathbf{G}_{\ell-1}) \mathbf{G}_\ell) \quad (19)$$

$$D_\ell = -\frac{\nu_\ell}{2} \log |\mathbf{K}(\mathbf{G}_{\ell-1})| \quad (20)$$

While we might think we need to know the features, \mathbf{F}_ℓ and $\mathbf{F}_{\ell-1}$ to evaluate $P(\mathbf{F}_\ell | \mathbf{F}_{\ell-1})$, in actuality, we

only need the Gram matrices, \mathbf{G}_ℓ and $\mathbf{G}_{\ell-1}$ (this is both because Eq. (19) can be rearranged using properties of the trace such that it depends only on \mathbf{G}_ℓ , and because the kernel can be written in terms of the previous Gram matrix). However, this objective still has its optimum at zero,

$$\mathbf{0} = \arg \max_{\mathbf{G}_\ell} [\log P(\mathbf{F}_\ell | \mathbf{F}_{\ell-1})]. \quad (21)$$

so it again does not satisfy our requirement (Eq. 16). Although, at least this objective is not pathological as the gradient is zero at $\mathbf{G}_\ell = \mathbf{0}$ unlike the $\log P(\mathbf{G}_\ell | \mathbf{G}_{\ell-1})$.

Instead, we need to consider an alternative objective, which can be obtained using two complementary approaches (Appendix B). First, we can consider the expected dynamics of Langevin sampling for a deep kernel process as gradient descent under a loss. Second, we can consider a modified ‘‘prior’’ which, when added to a conjugate log-likelihood, has a mode at the location of the posterior expectation. This objective mirrors MAP for features (Eq. 18),

$$\mathcal{L}_M(\mathbf{G}_\ell; \mathbf{G}_{\ell-1}) = \frac{\nu_\ell}{2} \log |\mathbf{G}_\ell| + T_\ell + D_\ell. \quad (22)$$

where T_ℓ and D_ℓ are defined in Eq. (19) and Eq. (20). Importantly though, this objective has an extra term, $\frac{\nu_\ell}{2} \log |\mathbf{G}_\ell|$, which encourages larger values of \mathbf{G}_ℓ and hence pushes the mode away from zero. As such, this objective does have the desired mode,

$$\mathbf{K}(\mathbf{G}_{\ell-1}) = \arg \max_{\mathbf{G}_\ell} [\mathcal{L}_M(\mathbf{G}_\ell; \mathbf{G}_{\ell-1})]. \quad (23)$$

4 Methods: Optimization

Before we begin in earnest, it is worth noting that we could optimize in the space of features, \mathbf{F}_ℓ and $\mathbf{F}_{\ell-1}$, or Gram matrices, \mathbf{G}_ℓ and $\mathbf{G}_{\ell-1}$. Optimizing features is standard, but there is strong reason to believe that optimizing Gram matrices might work better. In particular, note that the Gram matrix is invariant to unitary transformations in the features, $\mathbf{F}'_\ell = \mathbf{F}_\ell \mathbf{U}$, where $\mathbf{U} \in \mathbb{R}^{\nu_\ell \times \nu_\ell}$ satisfies $\mathbf{U} \mathbf{U}^T = \mathbf{I}$,

$$\mathbf{G}_\ell = \frac{1}{\nu_\ell} \mathbf{F}_\ell \mathbf{F}_\ell^T = \frac{1}{\nu_\ell} \mathbf{F}_\ell \mathbf{U} \mathbf{U}^T \mathbf{F}_\ell^T = \frac{1}{\nu_\ell} \mathbf{F}'_\ell \mathbf{F}'_\ell{}^T. \quad (24)$$

Thus, for every optimal Gram matrix, \mathbf{G}_ℓ , there is an infinite family of optimal features, \mathbf{F}_ℓ . This leads to a much more complex loss landscape, which is likely to be much more challenging to optimize (see Aitchison et al., 2021, for further details).

Now that we seek to explore optimizing Gram matrices, we encounter problems with standard gradient based optimization. In particular, we start by considering a simple, linear kernel,

$$\mathbf{K}(\mathbf{G}_{\ell-1}) = \mathbf{G}_{\ell-1}. \quad (25)$$

Isolating terms in the objective that depend on \mathbf{G}_ℓ ,

$$\mathcal{L}_M = T_\ell + D'_{\ell+1} + T_{\ell+1} + \text{const.} \quad (26)$$

where T_ℓ and $T_{\ell+1}$ is defined in Eq. (19), we have merged the $\frac{\nu_\ell}{2} \log |\mathbf{G}_\ell|$ and the $D_{\ell+1}$ terms to form $D'_{\ell+1}$,

$$\begin{aligned} D'_{\ell+1} &= \frac{\nu_\ell}{2} \log |\mathbf{G}_\ell| + D_{\ell+1} \\ &= \frac{\nu_\ell}{2} \log |\mathbf{G}_\ell| - \frac{\nu_{\ell+1}}{2} \log |\mathbf{K}(\mathbf{G}_\ell)|, \end{aligned} \quad (27)$$

and const includes all the other terms that do not depend either on \mathbf{G}_ℓ or $\mathbf{G}_{\ell-1}$. The gradients of each individual term are,

$$\frac{\partial T_\ell}{\partial \mathbf{G}_\ell} = -\frac{\nu_\ell}{2} \mathbf{G}_{\ell-1} \quad (28a)$$

$$\frac{\partial D'_{\ell+1}}{\partial \mathbf{G}_\ell} = \frac{\nu_\ell - \nu_{\ell+1}}{2} \mathbf{G}_\ell^{-1} \quad (28b)$$

$$\frac{\partial T_{\ell+1}}{\partial \mathbf{G}_\ell} = \frac{\nu_{\ell+1}}{2} \mathbf{G}_\ell^{-1} \mathbf{G}_{\ell+1} \mathbf{G}_\ell^{-1} \quad (28c)$$

And these gradients highlight the key issue with using gradient-based optimization. In particular, the gradient of $T_{\ell+1}$ is positive definite, whereas the gradient of T_ℓ is negative definite (the gradient of $D'_{\ell+1}$ can be positive definite, negative definite, or zero depending on $\nu_\ell - \nu_{\ell+1}$). Thus, on any given gradient step, the overall gradient will usually have some positive and some negative eigenvalues, in which case a large enough step size will result in an inadmissible, non-positive-definite Gram matrix. To resolve this issue, we need think considerably more carefully about the optimizer.

4.1 Exact solutions of the linear equations

Instead, note that for a linear kernel, there is a closed-form solution for the optimal value of \mathbf{G}_ℓ given fixed $\mathbf{G}_{\ell-1}$ and $\mathbf{G}_{\ell+1}$. In particular, our goal is to solve for the location where the gradient is zero,

$$\begin{aligned} \mathbf{0} &= \frac{\partial \mathcal{L}_M}{\partial \mathbf{G}_\ell} \\ \mathbf{0} &= \frac{\nu_\ell - \nu_{\ell+1}}{2} \mathbf{G}_\ell^{-1} - \frac{\nu_\ell}{2} \mathbf{G}_{\ell-1}^{-1} + \frac{\nu_{\ell+1}}{2} \mathbf{G}_\ell^{-1} \mathbf{G}_{\ell+1} \mathbf{G}_\ell^{-1}. \end{aligned} \quad (29)$$

These expressions are simplified by multiplying on both sides by \mathbf{G}_ℓ ,

$$\mathbf{0} = \frac{\nu_\ell - \nu_{\ell+1}}{2} \mathbf{G}_\ell - \frac{\nu_\ell}{2} \mathbf{G}_\ell \mathbf{G}_{\ell-1}^{-1} \mathbf{G}_\ell + \frac{\nu_{\ell+1}}{2} \mathbf{G}_{\ell+1}. \quad (30)$$

Observe that this is a CARE, as commonly used in control theory (Eq. 1), with,

$$\mathbf{A}_\ell = \frac{\nu_\ell - \nu_{\ell+1}}{4} \mathbf{I} \quad (31a)$$

$$\mathbf{U}_\ell = \frac{\nu_\ell}{2} \mathbf{G}_{\ell-1}^{-1} \quad (31b)$$

$$\mathbf{Q}_\ell = \frac{\nu_{\ell+1}}{2} \mathbf{G}_{\ell+1} \quad (31c)$$

This CARE can be solved in a single step using standard methods from control theory (Benner, 1999).

4.2 Writing the linear solution in terms of gradients

Of course, Eq. (31) is restricted to linear kernels. We therefore seek to adapt the exact linear solution to form an iterative solver for the nonlinear case. To strengthen our intuition, note that \mathbf{A}_ℓ arises from gradient of $D'_{\ell+1}$, \mathbf{U}_ℓ arises from the gradient of T_ℓ , and \mathbf{Q}_ℓ arises from the gradient of $T_{\ell+1}$. Thus, we could write \mathbf{A}_ℓ , \mathbf{U}_ℓ and \mathbf{Q}_ℓ in terms of these gradients,

$$\mathbf{A}_\ell = \frac{1}{2} \frac{\partial D'_{\ell+1}}{\partial \mathbf{G}_\ell} \Big|_{\tilde{\mathbf{G}}_\ell} \tilde{\mathbf{G}}_\ell \quad (32a)$$

$$\mathbf{U}_\ell = - \frac{\partial T_\ell}{\partial \mathbf{G}_\ell} \Big|_{\tilde{\mathbf{G}}_\ell} \quad (32b)$$

$$\mathbf{Q}_\ell = \tilde{\mathbf{G}}_\ell \frac{\partial T_{\ell+1}}{\partial \mathbf{G}_\ell} \Big|_{\tilde{\mathbf{G}}_\ell} \tilde{\mathbf{G}}_\ell \quad (32c)$$

where we now explicitly distinguish between the fixed value of the Gram matrix at the previous iteration, $\tilde{\mathbf{G}}_\ell$, and the variable over which we solve, \mathbf{G}_ℓ . Note that substituting the gradients for a linear kernel in Eq. (28) into Eq. (32) brings us back to the values of \mathbf{A}_ℓ , \mathbf{U}_ℓ and \mathbf{Q}_ℓ for linear kernels in Eq. (31). Importantly, these definitions of \mathbf{A}_ℓ , \mathbf{U}_ℓ and \mathbf{Q}_ℓ (Eq. 32) generalise directly to nonlinear kernels, suggesting that it might be possible to solve for the optimal Gram matrices by iteratively solving the CARE,

$$\mathbf{0} = \mathbf{A}_\ell^T \mathbf{G}_\ell + \mathbf{G}_\ell \mathbf{A}_\ell - \mathbf{G}_\ell \mathbf{U}_\ell \mathbf{G}_\ell + \mathbf{Q}_\ell. \quad (33)$$

However, we have yet to show that this CARE actually has a fixed point at the maximum of \mathcal{L}_M . To show that it does, we substitute \mathbf{A}_ℓ , \mathbf{U}_ℓ and \mathbf{Q}_ℓ (Eq. 32) into the CARE, which gives,

$$\begin{aligned} \mathbf{0} &= \mathbf{G}_\ell \frac{\partial T_\ell}{\partial \mathbf{G}_\ell} \Big|_{\tilde{\mathbf{G}}} \mathbf{G}_\ell + \tilde{\mathbf{G}}_\ell \frac{\partial T_{\ell+1}}{\partial \mathbf{G}_\ell} \Big|_{\tilde{\mathbf{G}}_\ell} \tilde{\mathbf{G}}_\ell \\ &\quad + \frac{1}{2} \left(\mathbf{G}_\ell \frac{\partial D'_{\ell+1}}{\partial \mathbf{G}_\ell} \Big|_{\tilde{\mathbf{G}}_\ell} \tilde{\mathbf{G}}_\ell + \tilde{\mathbf{G}}_\ell \frac{\partial D'_{\ell+1}}{\partial \mathbf{G}_\ell} \Big|_{\tilde{\mathbf{G}}_\ell} \mathbf{G}_\ell \right) \end{aligned} \quad (34)$$

Intuitively, this consists of each term in \mathcal{L}_M (Eq. 26), multiplied on the left and right by either \mathbf{G}_ℓ or $\tilde{\mathbf{G}}_\ell$. At a fixed point of iteratively solving the CARE (Eq. 33) we have $\mathbf{G}_\ell = \tilde{\mathbf{G}}_\ell$, so (Eq. 34) becomes,

$$\mathbf{0} = \mathbf{G}_\ell \left(\frac{\partial T_\ell}{\partial \mathbf{G}_\ell} + \frac{\partial T_{\ell+1}}{\partial \mathbf{G}_\ell} + \frac{\partial D'_{\ell+1}}{\partial \mathbf{G}_\ell} \right) \mathbf{G}_\ell \quad (35)$$

$$= \mathbf{G}_\ell \frac{\partial \mathcal{L}_M}{\partial \mathbf{G}_\ell} \mathbf{G}_\ell \quad (36)$$

which implies,

$$\mathbf{0} = \frac{\partial \mathcal{L}_M}{\partial \mathbf{G}_\ell}. \quad (37)$$

Algorithm 1 DKP solver

Parameters: $\{\nu_\ell\}_{\ell=1}^L$
Inputs: \mathbf{X}
Targets: \mathbf{Y}
 $\mathbf{G}_0 = \frac{1}{\nu_0} \mathbf{X} \mathbf{X}^T$
 $\mathbf{G}_{L+1} = \frac{1}{\nu_{L+1}} \mathbf{Y} \mathbf{Y}^T$
 initialize kernels from the prior
for ℓ **in** $(1, \dots, L)$ **do**
 $\mathbf{K}_{\ell-1} = \mathbf{K}(\mathbf{G}_{\ell-1})$
 $\mathbf{G}_\ell = \mathbf{K}_{\ell-1}$
end for
 solver
while not converged **do**
 for ℓ **in** $(L, \dots, 1)$ **do**
 compute terms in the objective
 $D'_{\ell+1} = \frac{\nu_\ell}{2} \log |\mathbf{G}_\ell| - \frac{\nu_{\ell+1}}{2} \log |\mathbf{K}(\mathbf{G}_\ell)|$
 $T_\ell = -\frac{\nu_\ell}{2} \text{Tr}(\mathbf{K}^{-1}(\mathbf{G}_{\ell-1}) \mathbf{G}_\ell)$
 $T_{\ell+1} = -\frac{\nu_{\ell+1}}{2} \text{Tr}(\mathbf{K}^{-1}(\mathbf{G}_\ell) \mathbf{G}_{\ell+1})$
 use autodiff to compute gradients
 $\mathbf{A}_\ell = \frac{1}{2} \frac{\partial D'_{\ell+1}}{\partial \mathbf{G}_\ell} \mathbf{G}_\ell$
 $\mathbf{U}_\ell = -\frac{\partial T_\ell}{\partial \mathbf{G}_\ell}$
 $\mathbf{Q}_\ell = \mathbf{G}_\ell \frac{\partial T_{\ell+1}}{\partial \mathbf{G}_\ell} \mathbf{G}_\ell$
 solve CARE
 $\mathbf{G}_\ell = \text{solve_care}(\mathbf{A}, \mathbf{U}, \mathbf{Q})$
 end for
end while

Thus, iteratively solving the CARE Eq. (33) does indeed have a fixed point at the maximum of our objective. For our full approach, see Alg. 4.2. Finally, we also use stabilisation strategies outlined in Appendix C and D.

5 Results

We considered a two hidden layer architecture, with a kernel inspired by the skip-connections used in (Salimbeni & Deisenroth, 2017). In particular, we used,

$$\mathbf{K}(\mathbf{G}_\ell) = w_1^\ell \mathbf{G}_\ell + w_2^\ell \mathbf{K}_{\text{sqexp}}(\mathbf{G}_\ell) \quad (38)$$

where w_1 and w_2 are hyperparameters learned by a Newton’s method, and $\mathbf{K}_{\text{sqexp}}(\mathbf{G}_\ell)$ is a standard squared-exponential kernel.

The algorithm as developed in this paper has $\mathcal{O}(P^3)$ scaling, where P is the number of datapoints, so we were forced to consider only the smallest UCI datasets from (Gal & Ghahramani, 2016). We started by confirming that optimizing our objective gives better performance than merely optimizing kernel hyperparameters, or than doing MAP inference with features (Eq. 18). We then go on to demonstrate that our solver is much faster than standard gradient based approaches (albeit restricted to these small datasets).

Table 1: RMSE after 10 solver iterations. (Equal best methods are displayed in bold. Error bars give two stderrs for a paired tests, which uses differences in performance between that method and best method, (so there are no meaningful error bars on the best performing method itself).

dataset	kernel hyper	features	\mathcal{L}_M
boston	2.79 ± 0.10	2.80 ± 0.08	2.67
concrete	5.47 ± 0.10	5.43 ± 0.11	5.17
energy	0.54 ± 0.01	0.48 \pm 0.02	0.47
yacht	0.80 ± 0.07	0.55	0.56 \pm 0.04

To begin, we compared the performance of our solver in three different settings. We considered a standard, kernel method mirror the structured of the deep kernel machine (Eq. 38) but where the only flexibility comes from the hyperparameters, w_1^ℓ , w_2^ℓ and σ^2 , as we set,

$$\mathbf{G}_\ell = \mathbf{K}(\mathbf{G}_{\ell-1}). \quad (39)$$

This method is denoted “kernel hyper” in Table 1. Next, we considered an objective given by MAP inference over features, \mathbf{F}_ℓ (Eq. 18), denoted “features”. Finally, we considered our objective, derived in Appendix B, and denoted \mathcal{L}_M . We found that simply optimizing the kernel hyperparameters gave considerably worse performance than using our objective in a deep kernel machine. In addition, we found that our objective gave a considerable improvement over MAP for features (Eq. 18) for boston and concrete, though the differences for energy and yacht were much smaller.

Finally, we compared the time required for our solver to that for gradient descent in Fig. 1. Our solver was considerably faster for all settings, except for boston and concrete with a learning rate of 0.01, which seems to track our solver, but then fail to reach the same rmse and either diverge (boston), or gets worse, and then much later gets better again (concrete). Energy and yacht are more stable.

We might be able to get better performance with more tuning of the learning rate (for instance, in boston and concrete, using a learning rate step at around 100 s). However, valid settings of the learning rate vary over many orders of magnitude, and the search space becomes huge as we start to consider learning rate decay schedules. This hyperparameter optimization process adds a considerable additional burden, which may well reduce or even eliminate the gains from fast convergence in the final run. In contrast, our method had two hyperparameters corresponding to the stabilisation strategies in Appendix C and D. Sensible values of these hyperparameters are in the range 1–10; we set $\lambda = 5$ and $\beta = 1$. Importantly, these were set to en-

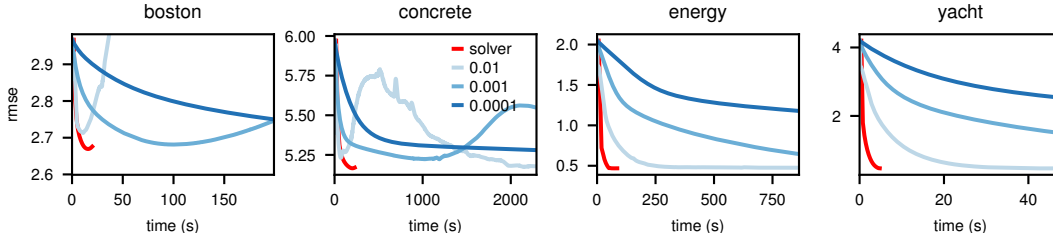


Figure 1: The root mean-squared error vs time for our solver (red) and gradient descent with Adam (blue) with different learning rates. The first row displays time on a linear axis, and the second row displays time on a logarithmic axis. Note that real compute times are a factor of 20 larger for all methods, as there are 20 splits for each dataset.

sure *stability* in one split of boston, entirely without reference to performance. These hyperparameter settings were then used without issue in all other splits for all other datasets, even with the feature objective (Eq. 18).

6 Related Work

The most closely related work is original work on Bayesian deep kernel methods, and in particular, deep kernel processes (Aitchison et al., 2021; Ober & Aitchison, 2021). Our work differs in that it introduces non-Bayesian deep kernel machines, which require a non-trivial objective, which is not simply e.g. MAP objective. In addition, this past work used slow inference algorithms based on gradient descent, whereas we develop fast solvers (though we are currently able to obtain only point estimates, rather than full approximate posteriors).

There is some work that uses proposes natural gradient methods for optimizing covariance matrices (Schmidt et al., 2021). However, this approach is fundamentally gradient based, so a CARE does not arise, and it does not reduce to the exact solution for linear kernels linear case. Importantly, our approach is fundamentally different from all (preconditioned/natural) gradient methods, which use the full gradient of the objective. In contrast, our approach exploits structure in the objective, and does different things with the gradient of different terms in the objective (Eq. 32).

While there is some work on highly flexible kernel hyperparameter optimization (e.g. Duvenaud et al., 2011; Duvenaud, 2014), this is very different from our deep kernel methods. In particular, these methods ultimately end up choosing a parametric kernel, and optimize the hyperparameters (even if they have a large search space over the parametric kernels). As such, these methods do not have the flexibility of neural networks and deep Gaussian processes. In contrast, Bayesian deep kernel processes generalise Bayesian

neural networks and deep Gaussian processes (Aitchison et al., 2021), so deep kernel methods do have the flexibility to compete with neural networks.

Finally, there are methods such as deep kernel learning (Wilson et al., 2016; Ober et al., 2021; Nikhitha et al., 2021) which combine a deep neural network with a standard, shallow kernel method such as a Gaussian process. While these methods are sometimes referred to as “deep kernel machines” (Nikhitha et al., 2021), we would argue that this term should be reserved for *purely* kernel-based methods, such as those introduced here, that do not involve any neural network-components.

7 Conclusion

We have introduced a new class of deep kernel method, the non-Bayesian deep kernel machine, and we introduced a loss function for the deep kernel machine, based on the expected dynamics of Langevin sampling (Appendix B). Next, we introduced a fast solver for deep kernel machines, which is radically different from standard (preconditioned/natural) gradient methods as it involves solving a CARE using methods from the control theory literature in the inner loop. In practice, the solver gives good predictive performance, and is considerably faster than equivalent gradient-descent based methods. While the current method is not yet scalable to many datapoints, it includes many fundamental ingredients that will enable the development of future scalable methods.

Acknowledgements

Thanks to Mahdiah Sadabadi and Jens Saak for discussing continuous time algebraic Ricatti equations and various solution strategies. Thanks to Adam Yang for proofreading the manuscript, and to Bristol’s Advanced Computing Research Centre (ACRC) for supporting computational resources.

References

- Laurence Aitchison. Why bigger is not always better: on finite and infinite neural networks. In *ICML*, 2020.
- Laurence Aitchison, Adam X. Yang, and Sebastian W. Ober. Deep kernel processes. In *ICML*, 2021.
- Peter Benner. Computational methods for linear-quadratic optimization. *Supplemento ai Rendiconti del Circolo Matematico di Palermo, Serie II*, No. 58:21–56, 1999. Extended version available as *Berichte aus der Technomathematik*, Report 98–04, Universität Bremen, August 1998, from <http://www.math.uni-bremen.de/zetem/berichte.html>.
- Taras Bodnar and Yarema Okhrin. Properties of the singular, inverse and generalized inverse partitioned wishart distributions. *Journal of Multivariate Analysis*, 99(10):2389–2405, 2008.
- Youngmin Cho and Lawrence K Saul. Kernel methods for deep learning. In *NeurIPS*, 2009.
- David Duvenaud. *Automatic model construction with Gaussian processes*. PhD thesis, University of Cambridge, 2014.
- David Duvenaud, Hannes Nickisch, and Carl Edward Rasmussen. Additive gaussian processes. *arXiv preprint arXiv:1112.4394*, 2011.
- Morris L Eaton et al. The Wishart distribution. In *Multivariate Statistics*, pp. 302–333. Institute of Mathematical Statistics, 2007.
- Yarin Gal and Zoubin Ghahramani. Dropout as a bayesian approximation: Representing model uncertainty in deep learning. In *international conference on machine learning*, pp. 1050–1059. PMLR, 2016.
- Thomas Hofmann, Bernhard Schölkopf, and Alexander J Smola. Kernel methods in machine learning. *The annals of statistics*, pp. 1171–1220, 2008.
- David Kleinman. On an iterative technique for riccati equation computations. *IEEE Transactions on Automatic Control*, 13(1):114–115, 1968.
- Alex Krizhevsky, Ilya Sutskever, and Geoffrey E. Hinton. Imagenet classification with deep convolutional neural networks. In *NIPS*, pp. 1106–1114, 2012.
- Peter Lancaster and Leiba Rodman. *Algebraic riccati equations*. Clarendon press, 1995.
- Nair K Nikhitha, AL Afzal, and S Asharaf. Deep kernel machines: a survey. *Pattern Analysis and Applications*, 24(2):537–556, 2021.
- Sebastian W. Ober and Laurence Aitchison. A variational approximate posterior for the deep Wishart process. *arXiv*, 2107.10125, 2021.
- Sebastian W Ober, Carl E Rasmussen, and Mark van der Wilk. The promises and pitfalls of deep kernel learning. *arXiv preprint arXiv:2102.12108*, 2021.
- Hugh Salimbeni and Marc Deisenroth. Doubly stochastic variational inference for deep gaussian processes. In *Advances in Neural Information Processing Systems*, pp. 4588–4599, 2017.
- Robin M Schmidt, Frank Schneider, and Philipp Hennig. Descending through a crowded valley — benchmarking deep learning optimizers. In *ICML*, 2021.
- John Shawe-Taylor and Nello Cristianini. *Kernel methods for pattern analysis*. Cambridge university press, 2004.
- Alex J Smola and Bernhard Schölkopf. *Learning with kernels*. MIT Press, 1998.
- Muni S Srivastava et al. Singular wishart and multivariate beta distributions. *The Annals of Statistics*, 31(5):1537–1560, 2003.
- Harald Uhlig. On singular wishart and singular multivariate beta distributions. *The Annals of Statistics*, pp. 395–405, 1994.
- Florian Wenzel, Kevin Roth, Bastiaan S Veeling, Jakub Swiatkowski, Linh Tran, Stephan Mandt, Jasper Snoek, Tim Salimans, Rodolphe Jenatton, and Sebastian Nowozin. How good is the bayes posterior in deep neural networks really? *arXiv preprint arXiv:2002.02405*, 2020.
- Andrew Gordon Wilson, Zhiting Hu, Ruslan Salakhutdinov, and Eric P Xing. Deep kernel learning. In *Artificial intelligence and statistics*, pp. 370–378. PMLR, 2016.

A Properties and pathologies of the singular Wishart

As we are dealing with a Wishart process, the number of input points is unbounded, so there is always the possibility that $\nu < P$ and sampled Gram matrices are singular. In that case, we need to be careful about understanding properties of the Wishart distribution. The probability density of the singular Wishart (with $\nu \leq P$) is, (Uhlrig, 1994; Srivastava et al., 2003; Bodnar & Okhrin, 2008).

$$\log P(\mathbf{X}) = \frac{1}{2}(\nu - p - 1) \log |\mathbf{X}_{:\nu,:\nu}| - \frac{1}{2} \text{Tr}(\mathbf{X}) + \text{const.} \quad (40)$$

where $\mathbf{X}_{:\nu,:\nu}$ is the top-left $\nu \times \nu$ submatrix. To compute the mode, we maximize over \mathbf{X} . Usually, we would do this by finding the location at which the gradient is zero,

$$\mathbf{0} = \frac{\partial \log P(\mathbf{X})}{\partial \mathbf{X}_{:\nu,:\nu}} = \frac{1}{2}(\nu - p - 1) \mathbf{X}_{:\nu,:\nu}^{-1} - \frac{1}{2} \mathbf{I} \quad (41)$$

$$\mathbf{X}_{:\nu,:\nu} = -\frac{1}{p+1-\nu} \mathbf{I} \quad (42)$$

However, as $\mathbf{X}_{:\nu,:\nu}$ is positive definite, this gradient is always negative definite, which would imply that the mode is at $\mathbf{X} = \mathbf{0}$. But things get worse — as $\mathbf{X}_{:\nu,:\nu} \rightarrow \mathbf{0}$, the gradient explodes due to the $\mathbf{X}_{:\nu,:\nu}^{-1}$ term. Thus, the objective is highly pathological, and thus not at all suitable for use as the objective for a deep kernel machine.

B Mean objectives

As discussed in Appendix A, there is always the possibility that $\nu < P$, in which case the mode of the prior is zero, and if the likelihood is sufficiently weak, the mode of the posterior will also be zero. Thus, if we are still to obtain a useful point estimate by maximizing an objective, we need to choose a different objective. There are two ways to derive this distribution, and we consider both here.

B.1 Capturing the posterior mean with conjugate likelihoods

Here we define a “mean objective”, \mathcal{M} , who’s mode gives the expected value. In the ideal case, the mode of the mean objective plus a log-likelihood would give the expectation of the posterior. While this cannot hold in general, we are able to guarantee it for conjugate likelihoods in the full-rank case (i.e. for $P \leq \nu$).

We begin by using the standard Wishart parameterisation, and noting that the mean is different from the mode,

$$\mathbf{X} \sim \mathcal{W}(\mathbf{\Sigma}, \nu), \quad (43)$$

$$\log \mathcal{W}(\mathbf{X}; \mathbf{\Sigma}, \nu) = \frac{\nu - P - 1}{2} \log |\mathbf{X}| - \frac{1}{2} \text{Tr}(\mathbf{\Sigma}^{-1} \mathbf{X}) + \text{const}, \quad (44)$$

$$\mathbb{E}[\mathbf{X}] = \nu \mathbf{\Sigma}, \quad (45)$$

$$\arg \max_{\mathbf{X}} [\mathcal{W}(\mathbf{X}; \mathbf{\Sigma}, \nu)] = (\nu - P - 1) \mathbf{\Sigma}. \quad (46)$$

Note that the expectation (Eq. 45) is true for the low-rank and full-rank case, as it can be derived by constructing the Wishart sample from outer products of Gaussian distributed vectors. But the expression for the probability density function (Eq. 44) is valid only when $P \leq \nu$, and the expression for the mode (Eq. 44) is valid only when $P \leq \nu + 1$. For the Wishart, we use a mean objective of form,

$$\mathcal{M}(\mathbf{X}; \mathbf{\Sigma}, \nu) = \frac{\nu}{2} \log |\mathbf{X}| - \frac{1}{2} \text{Tr}(\mathbf{\Sigma}^{-1} \mathbf{X}). \quad (47)$$

As hoped, the mode of the mean objective is equal to the prior expectation,

$$\frac{\partial \mathcal{M}(\mathbf{X}; \mathbf{\Sigma}, \nu)}{\partial \mathbf{X}^{-1}} = \frac{\nu}{2} \mathbf{X}^{-1} - \frac{1}{2} \mathbf{\Sigma}^{-1}, \quad (48)$$

$$\arg \max_{\mathbf{X}} [\mathcal{M}(\mathbf{X}; \mathbf{\Sigma}, \nu)] = \nu \mathbf{\Sigma} = \mathbb{E}[\mathbf{X}]. \quad (49)$$

Next, consider a conjugate likelihood, formed by a Gaussian, with N observed vectors, \mathbf{y}_λ forming a matrix, $\mathbf{Y} = (\mathbf{y}_1 \cdots \mathbf{y}_N)$, with \mathbf{X} being the precision,

$$\log P(\mathbf{Y}|\mathbf{X}) = \log \mathcal{N}(\mathbf{Y}; \mathbf{0}, \mathbf{X}^{-1}) = \frac{N}{2} \log |\mathbf{X}| - \text{Tr}(\mathbf{X} \mathbf{Y} \mathbf{Y}^T) + \text{const.} \quad (50)$$

The resulting conditional distribution is,

$$\log P(\mathbf{X}|\mathbf{Y}) = \log P(\mathbf{X}) + \log P(\mathbf{Y}|\mathbf{X}) + \text{const} \quad (51)$$

$$= \frac{(N+\nu)-P-1}{2} \log |\mathbf{X}| - \frac{1}{2} \text{Tr}((\mathbf{\Sigma}^{-1} + \mathbf{Y}\mathbf{Y}^T) \mathbf{X}) + \text{const} \quad (52)$$

$$= \log \mathcal{W}(\mathbf{X}; (\mathbf{\Sigma}^{-1} + \mathbf{Y}\mathbf{Y}^T)^{-1}, N + \nu). \quad (53)$$

The conditional mean is thus,

$$\mathbb{E}[\mathbf{X}|\mathbf{Y}] = (N + \nu) (\mathbf{\Sigma}^{-1} + \mathbf{Y}\mathbf{Y}^T)^{-1}. \quad (54)$$

The mean objective plus the likelihood is,

$$\mathcal{M}(\mathbf{X}; \mathbf{\Sigma}, \nu) + \log P(\mathbf{Y}|\mathbf{X}) = \frac{\nu+N}{2} \log |\mathbf{X}| - \frac{1}{2} \text{Tr}((\mathbf{\Sigma}^{-1} + \mathbf{Y}\mathbf{Y}^T) \mathbf{X}) + \text{const}.$$

Optimizing this objective, without restricting ourselves to low-rank \mathbf{X} , we get back the conditional expectation,

$$\arg \max_{\mathbf{X}} [\mathcal{M}(\mathbf{X}; \mathbf{\Sigma}, \nu) + \log P(\mathbf{Y}|\mathbf{X})] = (N + \nu) (\mathbf{\Sigma}^{-1} + \mathbf{Y}\mathbf{Y}^T)^{-1} = \mathbb{E}[\mathbf{X}|\mathbf{Y}], \quad (55)$$

as required.

Finally, as discussed in Appendix A, we are generally interested in the low-rank case for which $\nu < P$. Interestingly, if we optimize over \mathbf{X} in the space of all positive definite matrices, then the mode of the mean objective (Eq. 49) is still equal to the prior expectation. This is a bit odd, because samples, \mathbf{X} from the distribution are low-rank, but in the optimization we allow \mathbf{X} to be full rank. But it is a perfectly sensible choice because we are ultimately interested in characterising the posterior mean, and the posterior mean is itself usually full-rank. That said, extending the argument about conjugate likelihoods to the singular case is more difficult, as it is not clear exactly how to define such a conjugate likelihood.

B.2 Wishart by Langevin sampling

As an alternative approach, consider Langevin sampling on the underlying Gaussian distributed features, $\mathbf{F} \in \mathbb{R}^{P \times \nu_\ell}$, where ν_ℓ is the hidden-layer dimension and P is the number of datapoints. Note that we suppress the layer index, ℓ , on \mathbf{F} for simplicity, but we could in principle consider one set of features \mathbf{F}_ℓ for each layer. Thus, the Gram matrix can be written as,

$$\mathbf{G}_\ell = \frac{1}{\nu_\ell} \mathbf{F}\mathbf{F}^T \in \mathbb{R}^{P \times P}. \quad (56)$$

To infer \mathbf{F} , we use the joint log-probability,

$$\mathcal{J} = \log P(\mathbf{F}, \mathbf{G}_{\ell+1} | \mathbf{G}_{\ell-1}) \quad (57)$$

$$= \log P(\mathbf{F} | \mathbf{G}_{\ell-1}) + \log P\left(\mathbf{G}_{\ell+1} | \mathbf{G}_\ell = \frac{1}{\nu_\ell} \mathbf{F}\mathbf{F}^T\right) \quad (58)$$

$$= -\frac{1}{2} \text{Tr}(\mathbf{F}\mathbf{F}^T \mathbf{K}_\ell^{-1} (\mathbf{G}_{\ell-1})) + \log P\left(\mathbf{G}_{\ell+1} \middle| \mathbf{G}_\ell = \frac{1}{\nu_\ell} \mathbf{F}\mathbf{F}^T\right) + \text{const}. \quad (59)$$

Eventually, we will exploit the fact that this joint probability can be written entirely in terms of \mathbf{G}_ℓ ,

$$\mathcal{J} = -\frac{\nu_\ell}{2} \text{Tr}(\mathbf{G}_\ell \mathbf{K}_\ell^{-1} (\mathbf{G}_{\ell-1})) + \log P(\mathbf{G}_{\ell+1} | \mathbf{G}_\ell) + \text{const}. \quad (60)$$

Importantly, note even though we write \mathcal{J} in terms of \mathbf{G}_ℓ , it still gives the probability density for the distribution over \mathbf{F} .

To infer \mathbf{G}_ℓ , we consider doing Langevin sampling for \mathbf{F} ,

$$d\mathbf{F} = \frac{1}{2} dt \frac{\partial \mathcal{J}}{\partial \mathbf{F}} + d\mathbf{\Xi}, \quad (61)$$

where $d\Xi$ can be understood as IID Gaussian noise (formally, it is the differential of a matrix-valued Wiener process). Thus, the expected update to \mathbf{G} can be written,

$$\mathbb{E}[d\mathbf{G}_\ell | \mathbf{G}_{\ell-1}, \mathbf{F}, \mathbf{G}_{\ell+1}] = \frac{1}{\nu_\ell} d(\mathbf{F}\mathbf{F}^T) \quad (62)$$

$$= \frac{1}{2\nu_\ell} dt \left(\left(\frac{\partial \mathcal{J}}{\partial \mathbf{F}} \right) \mathbf{F}^T + \mathbf{F} \left(\frac{\partial \mathcal{J}}{\partial \mathbf{F}} \right)^T \right) + \frac{1}{\nu_\ell} \mathbb{E}[d\Xi d\Xi^T]. \quad (63)$$

The last term is,

$$\frac{1}{\nu_\ell} \mathbb{E}[d\Xi d\Xi^T] = dt \mathbf{I}, \quad (64)$$

So,

$$\mathbb{E}[d\mathbf{G}_\ell | \mathbf{G}_{\ell-1}, \mathbf{F}, \mathbf{G}_{\ell+1}] = \frac{1}{2\nu_\ell} dt \left(\left(\frac{\partial \mathcal{J}}{\partial \mathbf{F}} \right) \mathbf{F}^T + \mathbf{F} \left(\frac{\partial \mathcal{J}}{\partial \mathbf{F}} \right)^T \right) + dt \mathbf{I} \quad (65)$$

Now, we write $\frac{\partial \mathcal{J}}{\partial \mathbf{F}}$ in terms of $\frac{\partial \mathcal{J}}{\partial \mathbf{G}}$,

$$\frac{\partial \mathcal{J}}{\partial F_{\alpha\beta}} = \sum_{ij} \frac{\partial \mathcal{J}}{\partial G_{ij}^\ell} \frac{\partial G_{ij}^\ell}{\partial F_{\alpha\beta}} \quad (66)$$

$$= \frac{1}{\nu_\ell} \sum_{ij} \frac{\partial \mathcal{J}}{\partial G_{ij}^\ell} \frac{\partial}{\partial F_{\alpha\beta}} \sum_k F_{ik} F_{jk} \quad (67)$$

$$= \frac{1}{\nu_\ell} \sum_{ij} \frac{\partial \mathcal{J}}{\partial G_{ij}^\ell} \frac{\partial}{\partial F_{\alpha\beta}} \sum_k (\delta_{\alpha i} \delta_{\beta k} F_{jk} + F_{ik} \delta_{\alpha j} \delta_{\beta k}) \quad (68)$$

$$= \frac{1}{\nu_\ell} \left(\sum_j \frac{\partial \mathcal{J}}{\partial G_{\alpha j}^\ell} F_{j\beta} + \sum_i \frac{\partial \mathcal{J}}{\partial G_{i\alpha}^\ell} F_{i\beta} \right), \quad (69)$$

As the gradient of \mathcal{J} wrt \mathbf{G} is symmetric,

$$\frac{\partial \mathcal{J}}{\partial \mathbf{F}} = \frac{2}{\nu_\ell} \frac{\partial \mathcal{J}}{\partial \mathbf{G}} \mathbf{F}. \quad (70)$$

Thus, we can rewrite the expected updates for \mathbf{G}_ℓ entirely in terms of \mathbf{G}_ℓ and not in terms of \mathbf{F} ,

$$\mathbb{E}[d\mathbf{G}_\ell | \mathbf{G}_{\ell-1}, \mathbf{F}, \mathbf{G}_{\ell+1}] = \frac{1}{\nu_\ell^2} dt \left(\frac{\partial \mathcal{J}}{\partial \mathbf{G}_\ell} \mathbf{F}\mathbf{F}^T + \mathbf{F}\mathbf{F}^T \frac{\partial \mathcal{J}}{\partial \mathbf{G}_\ell} \right) + dt \mathbf{I} \quad (71)$$

$$\mathbb{E}[d\mathbf{G}_\ell | \mathbf{G}_{\ell-1}, \mathbf{G}_\ell, \mathbf{G}_{\ell+1}] = \frac{1}{\nu_\ell} dt \left(\frac{\partial \mathcal{J}}{\partial \mathbf{G}_\ell} \mathbf{G}_\ell + \mathbf{G}_\ell \frac{\partial \mathcal{J}}{\partial \mathbf{G}_\ell} \right) + dt \mathbf{I}. \quad (72)$$

Now that we understand the dynamics expected under Langevin sampling, we define a new matrix, $\bar{\mathbf{G}}$ following these dynamics,

$$d\bar{\mathbf{G}}_\ell = \left(\frac{1}{\nu_\ell} \left(\frac{\partial \bar{\mathcal{J}}}{\partial \bar{\mathbf{G}}_\ell} \bar{\mathbf{G}}_\ell + \bar{\mathbf{G}}_\ell \frac{\partial \bar{\mathcal{J}}}{\partial \bar{\mathbf{G}}_\ell} \right) + \mathbf{I} \right) dt, \quad (73)$$

where $\bar{\mathcal{J}}$ is just Eq. 60, where $\bar{\mathbf{G}}_\ell$ replaces \mathbf{G}_ℓ ,

$$\bar{\mathcal{J}} = -\frac{\nu_\ell}{2} \text{Tr}(\bar{\mathbf{G}}_\ell \mathbf{K}_\ell^{-1} (\mathbf{G}_{\ell-1})) + \log P(\mathbf{G}_{\ell+1} | \mathbf{G}_\ell = \bar{\mathbf{G}}_\ell) + \text{const}. \quad (74)$$

Importantly, $\bar{\mathbf{G}}_\ell$ will be full rank due to the $+dt \mathbf{I}$ term in the dynamics (Eq. 73).

Now, we seek to interpret these expected Langevin dynamics as preconditioned gradient descent under a modified loss. In particular, as $\bar{\mathbf{G}}_\ell$ is full rank, it makes sense to consider the following objective,

$$\mathcal{L} = \bar{\mathcal{J}} + \frac{\nu_\ell}{2} \log |\bar{\mathbf{G}}_\ell| \quad (75)$$

$$\frac{\partial \mathcal{L}}{\partial \bar{\mathbf{G}}_\ell} = \frac{\partial \bar{\mathcal{J}}}{\partial \bar{\mathbf{G}}_\ell} + \frac{\nu_\ell}{2} \bar{\mathbf{G}}_\ell^{-1} \quad (76)$$

We then precondition using the positive definite matrix, $\frac{1}{\nu_\ell} (\bar{\mathbf{G}}_\ell \otimes \mathbf{I} + \mathbf{I} \otimes \bar{\mathbf{G}}_\ell)$,

$$\frac{1}{\nu_\ell} (\bar{\mathbf{G}}_\ell \otimes \mathbf{I} + \mathbf{I} \otimes \bar{\mathbf{G}}_\ell) \text{vec} \left(\frac{\partial \mathcal{L}}{\partial \bar{\mathbf{G}}_\ell} \right) = (\bar{\mathbf{G}}_\ell \otimes \mathbf{I} + \mathbf{I} \otimes \bar{\mathbf{G}}_\ell) \text{vec} \left(\frac{1}{\nu_\ell} \frac{\partial \bar{\mathcal{J}}}{\partial \bar{\mathbf{G}}_\ell} + \frac{1}{2} \bar{\mathbf{G}}_\ell^{-1} \right) \quad (77)$$

$$= \text{vec} \left(\frac{1}{\nu_\ell} \left(\frac{\partial \bar{\mathcal{J}}}{\partial \bar{\mathbf{G}}_\ell} \bar{\mathbf{G}}_\ell + \bar{\mathbf{G}}_\ell \frac{\partial \bar{\mathcal{J}}}{\partial \bar{\mathbf{G}}_\ell} \right) + \mathbf{I} \right). \quad (78)$$

This is equivalent to Eq. (73), so optimizing Eq. (75) indeed finds the approximate expectation arising from Langevin sampling.

The full objective is thus,

$$\mathcal{L}_M = \underbrace{-\frac{\nu_\ell}{2} \text{Tr} (\bar{\mathbf{G}}_\ell \mathbf{K}_\ell^{-1}) + \frac{\nu_\ell}{2} \log |\bar{\mathbf{G}}_\ell|}_{=\mathcal{M}} + \log P (\mathbf{G}_{\ell+1} | \mathbf{G}_\ell = \bar{\mathbf{G}}_\ell) + \text{const.} \quad (79)$$

where the first part can be interpreted as a mean objective, equivalent to that derived in Appendix. B.1.

C Solving the CARE as preconditioned gradient-based optimization

Solving the CARE in Eq. 33 still seems a bit mysterious: it certainly is not equivalent to the gradient-based strategies that we are used to. Indeed, many strategies exist for solving the CARE, and many of them do not correspond to gradient-based optimization as we usually understand it. However, one strategy — Kleinman’s Newton’s method (Kleinman, 1968) — does correspond to gradient-based optimization. Kleinman’s Newton’s method begins by writing \mathbf{G}_ℓ in terms of the previous iterate, $\tilde{\mathbf{G}}_\ell$, and a perturbation, $\delta \mathbf{G}_\ell$,

$$\mathbf{G}_\ell = \tilde{\mathbf{G}}_\ell + \delta \mathbf{G}_\ell \quad (80)$$

Substituting this form for \mathbf{G}_ℓ into Eq. (33) gives, a Lyapunov equation that can be solved directly using e.g. routines in SciPy,

$$\mathbf{0} = \left(\mathbf{Q} + \mathbf{A}^T \tilde{\mathbf{G}}_\ell + \mathbf{A} \tilde{\mathbf{G}}_\ell - \tilde{\mathbf{G}}_\ell \mathbf{U} \tilde{\mathbf{G}}_\ell \right) + \delta \mathbf{G}_\ell \left(\mathbf{A}_\ell - \mathbf{U}_\ell \tilde{\mathbf{G}}_\ell \right) + \left(\mathbf{A}_\ell - \mathbf{U}_\ell \tilde{\mathbf{G}}_\ell \right)^T \delta \mathbf{G}_\ell \quad (81)$$

However, to solve this equation, we require that the real part of all eigenvalues of

$$\mathbf{A}_{\text{lyap}} = \mathbf{A}_\ell - \mathbf{U}_\ell \tilde{\mathbf{G}}_\ell \quad (82)$$

is negative. As this does not always hold, we can modify Newton’s Kleinman’s method (without changing the fixed points), by using,

$$\mathbf{0} = \left(\mathbf{Q} + \mathbf{A}^T \tilde{\mathbf{G}}_\ell + \mathbf{A} \tilde{\mathbf{G}}_\ell - \tilde{\mathbf{G}}_\ell \mathbf{U} \tilde{\mathbf{G}}_\ell \right) + \delta \mathbf{G}_\ell \left(\mathbf{A}_\ell - \mathbf{U}_\ell \tilde{\mathbf{G}}_\ell - \beta \mathbf{I} \right) + \left(\mathbf{A}_\ell - \mathbf{U}_\ell \tilde{\mathbf{G}}_\ell - \beta \mathbf{I} \right)^T \delta \mathbf{G}_\ell \quad (83)$$

In that case, we have

$$\mathbf{A}_{\text{lyap}} = \mathbf{A}_\ell - \mathbf{U}_\ell \tilde{\mathbf{G}}_\ell - \beta \mathbf{I} \quad (84)$$

And it is always possible to set β large enough to ensure that the real parts of all eigenvalues of \mathbf{A}_{lyap} negative. In practice, we use $\beta = 1$.

D Proximal gradient descent like objectives

Mirroring proximal gradient descent, we stabilise the solution by including a regulariser in the objective, to ensure the mode is not too far from the previous mode. In particular, we measure the discrepancy between \mathbf{G}_ℓ and $\tilde{\mathbf{G}}_\ell$ using,

$$d_\ell = -\text{Tr} \left(\mathbf{G}_\ell \tilde{\mathbf{G}}_\ell^{-1} \right) - \text{Tr} \left(\mathbf{G}_\ell^{-1} \tilde{\mathbf{G}}_\ell \right). \quad (85)$$

Importantly, this has a maximum at $\mathbf{G}_\ell = \tilde{\mathbf{G}}_\ell$,

$$\mathbf{0} = \frac{\partial d_\ell}{\partial \mathbf{G}_\ell} = -\tilde{\mathbf{G}}_\ell^{-1} + \mathbf{G}_\ell^{-1} \tilde{\mathbf{G}} \mathbf{G}_\ell^{-1}. \quad (86)$$

Mirroring the approach we take for linear kernels (Eq.), to include these terms in the objective, we need to multiply on both sides by \mathbf{G}_ℓ

$$\mathbf{G}_\ell \frac{\partial d_\ell}{\partial \mathbf{G}_\ell} \mathbf{G}_\ell = -\mathbf{G}_\ell \tilde{\mathbf{G}}_\ell^{-1} \mathbf{G}_\ell + \tilde{\mathbf{G}}_\ell \quad (87)$$

Thus, if we seek to optimize $\mathcal{L}_M + \lambda d_\ell$, we get a CARE with,

$$\mathbf{A}_\ell = \frac{1}{2} \frac{\partial D_{\ell+1}}{\partial \mathbf{G}_\ell} \Big|_{\tilde{\mathbf{G}}_\ell} \tilde{\mathbf{G}}_\ell \quad (88)$$

$$\mathbf{U}_\ell = - \frac{\partial T_\ell}{\partial \mathbf{G}_\ell} \Big|_{\tilde{\mathbf{G}}_\ell} + \lambda \tilde{\mathbf{G}}_\ell^{-1} \quad (89)$$

$$\mathbf{Q}_\ell = \tilde{\mathbf{G}}_\ell \frac{\partial T_{\ell+1}}{\partial \mathbf{G}_\ell} \Big|_{\tilde{\mathbf{G}}_\ell} \tilde{\mathbf{G}}_\ell + \lambda \tilde{\mathbf{G}} \quad (90)$$

E Prediction

Our goal is to predict the full Gram matrix,

$$\mathbf{G}_\ell = \begin{pmatrix} \mathbf{G}_{ii}^\ell & \mathbf{G}_{it}^\ell \\ \mathbf{G}_{ti}^\ell & \mathbf{G}_{tt}^\ell \end{pmatrix} \quad (91)$$

for both test points (labelled “t”) and training points (labelled “i”) from just the training points. For clarity, we have $\mathbf{G}_\ell \in \mathbb{R}^{P \times P}$, $\mathbf{G}_{ii}^\ell \in \mathbb{R}^{P_i \times P_i}$, $\mathbf{G}_{ti}^\ell \in \mathbb{R}^{P_t \times P_i}$, $\mathbf{G}_{tt}^\ell \in \mathbb{R}^{P_t \times P_t}$, where P_i is the number of training points, P_t is the number of test points and $P = P_i + P_t$ is the total number of train and test points. Our goal is to estimate \mathbf{G}_{it}^ℓ and \mathbf{G}_{tt}^ℓ from \mathbf{G}_{ii}^ℓ .

To address this issue, we follow the approach taken in (Ober & Aitchison, 2021) by writing the Gram matrix in terms of Gaussian-distributed features,

$$\mathbf{F}_\ell \mathbf{F}_\ell^T = \nu \mathbf{G}_\ell \sim \mathcal{W}(\mathbf{K}_\ell(\mathbf{G}_{\ell-1}), \nu), \quad (92)$$

with

$$\mathbf{F}_\ell = \begin{pmatrix} \mathbf{F}_i^\ell \\ \mathbf{F}_t^\ell \end{pmatrix} \quad \mathbf{K}_\ell(\mathbf{G}_{\ell-1}) = \begin{pmatrix} \mathbf{K}_{ii} & \mathbf{K}_{ti}^T \\ \mathbf{K}_{ti} & \mathbf{K}_{tt} \end{pmatrix} \quad (93)$$

where $\mathbf{F}_\ell \in \mathbb{R}^{(P_i+P_t) \times \nu_\ell}$, $\mathbf{F}_i \in \mathbb{R}^{P_i \times \nu_\ell}$ and $\mathbf{F}_t \in \mathbb{R}^{P_t \times \nu_\ell}$. Critically, \mathbf{F}_t conditioned on \mathbf{F}_i is given by a matrix normal, (Eaton et al., 2007, page 310),

$$\mathbf{P}(\mathbf{F}_t^\ell | \mathbf{F}_i^\ell) = \mathcal{MN}(\mathbf{K}_{ti} \mathbf{K}_{ii}^{-1} \mathbf{F}_i, \mathbf{K}_{tt \cdot i}, \mathbf{I}), \quad (94)$$

where

$$\mathbf{K}_{tt \cdot i} = \mathbf{K}_{tt} - \mathbf{K}_{it}^T \mathbf{K}_{ii}^{-1} \mathbf{K}_{it}. \quad (95)$$

Then \mathbf{G}_ℓ , which includes \mathbf{G}_{it}^ℓ and \mathbf{G}_{tt}^ℓ is given by,

$$\mathbf{G}_\ell = \begin{pmatrix} \mathbf{G}_{ii}^\ell & \mathbf{G}_{it}^\ell \\ \mathbf{G}_{ti}^\ell & \mathbf{G}_{tt}^\ell \end{pmatrix} = \frac{1}{\nu} \begin{pmatrix} \mathbf{F}_i^\ell (\mathbf{F}_i^\ell)^T & \mathbf{F}_i^\ell (\mathbf{F}_t^\ell)^T \\ \mathbf{F}_t^\ell (\mathbf{F}_i^\ell)^T & \mathbf{F}_t^\ell (\mathbf{F}_t^\ell)^T \end{pmatrix} = \frac{1}{\nu} \mathbf{F}_\ell \mathbf{F}_\ell^T \quad (96)$$

For \mathbf{F}_i , we can use any value as long as $\mathbf{G}_{ii}^\ell = \mathbf{F}_i^\ell (\mathbf{F}_i^\ell)^T$, as the resulting values of \mathbf{G}_{ti}^ℓ and \mathbf{G}_{tt}^ℓ will not depend on the specific choice of \mathbf{F}_i .

Algorithm 2 DKP prediction

Parameters: $\{\nu_\ell\}_{\ell=1}^L$
Gram matrices from solver in Alg. 4.2: $\{\mathbf{G}_{ii}^\ell\}_{\ell=1}^L$
Training and test inputs: $\mathbf{X}_i, \mathbf{X}_t$
Training targets: \mathbf{Y}_i

Initialize full Gram matrix

$$\begin{pmatrix} \mathbf{G}_{ii}^0 & \mathbf{G}_{ti}^{0;T} \\ \mathbf{G}_{ti}^0 & \mathbf{G}_{tt}^0 \end{pmatrix} = \frac{1}{\nu_0} \begin{pmatrix} \mathbf{X}_i \mathbf{X}_i^T & \mathbf{X}_i \mathbf{X}_t^T \\ \mathbf{X}_t \mathbf{X}_i^T & \mathbf{X}_t \mathbf{X}_t^T \end{pmatrix}$$

Propagate full Gram matrix

for ℓ **in** $(1, \dots, L)$ **do**

$$\begin{pmatrix} \mathbf{K}_{ii} & \mathbf{K}_{ti}^T \\ \mathbf{K}_{ti} & \mathbf{K}_{tt} \end{pmatrix} = \mathbf{K} \left(\begin{pmatrix} \mathbf{G}_{ii}^{\ell-1} & \mathbf{G}_{ti}^{\ell-1;T} \\ \mathbf{G}_{ti}^{\ell-1} & \mathbf{G}_{tt}^{\ell-1} \end{pmatrix} \right)$$

$$\mathbf{K}_{tt:i} = \mathbf{K}_{tt} - \mathbf{K}_{it}^T \mathbf{K}_{ii}^{-1} \mathbf{K}_{it}$$

$$\mathbf{G}_{ti}^\ell = \mathbf{K}_{ti}^T \mathbf{K}_{ii}^{-1} \mathbf{G}_{ii}^\ell$$

$$\mathbf{G}_{tt}^\ell = \mathbf{K}_{ti}^T \mathbf{K}_{ii}^{-1} \mathbf{G}_{ii}^\ell \mathbf{K}_{ii}^{-1} \mathbf{K}_{ti} + \mathbf{K}_{tt:i}$$

end for

Final prediction using standard Gaussian process expressions

$$\begin{pmatrix} \mathbf{K}_{ii} & \mathbf{K}_{ti}^T \\ \mathbf{K}_{ti} & \mathbf{K}_{tt} \end{pmatrix} = \mathbf{K} \left(\begin{pmatrix} \mathbf{G}_{ii}^L & \mathbf{G}_{ti}^{L;T} \\ \mathbf{G}_{ti}^L & \mathbf{G}_{tt}^L \end{pmatrix} \right) + \sigma^2 \mathbf{I}$$

$$\mathbf{Y}_t \sim \mathcal{N}(\mathbf{K}_{ti} \mathbf{K}_{ii}^{-1} \mathbf{Y}_i, \mathbf{K}_{tt} - \mathbf{K}_{ti} \mathbf{K}_{ii}^{-1} \mathbf{K}_{ti}^T)$$

In the deterministic case, we are interested in the expected value of \mathbf{G}_{it} and \mathbf{G}_{tt} . Given Eq. (94), we have

$$\mathbf{F}_t = \mathbf{K}_{ti} \mathbf{K}_{ii}^{-1} \mathbf{F}_i + \mathbf{K}_{tt:i}^{1/2} \boldsymbol{\Xi}. \quad (97)$$

where $\boldsymbol{\Xi}$ is a matrix with IID standard Gaussian elements. Thus,

$$\mathbf{G}_{ti} = \frac{1}{\nu} \mathbb{E} [\mathbf{F}_t \mathbf{F}_i^T] = \frac{1}{\nu} \mathbf{K}_{ti} \mathbf{K}_{ii}^{-1} \mathbf{F}_i \mathbf{F}_i^T = \mathbf{K}_{ti} \mathbf{K}_{ii}^{-1} \mathbf{G}_{ii} \quad (98)$$

We can do the same for $\mathbf{F}_t \mathbf{F}_t^T$:

$$\mathbf{G}_{tt} = \frac{1}{\nu} \mathbb{E} [\mathbf{F}_t \mathbf{F}_t^T] = \frac{1}{\nu} \mathbf{K}_{ti} \mathbf{K}_{ii}^{-1} \mathbb{E} [\mathbf{F}_i \mathbf{F}_i^T] \mathbf{K}_{ii}^{-1} \mathbf{K}_{ti}^T + \frac{1}{\nu} \mathbf{K}_{tt:i}^{1/2} \mathbb{E} [\boldsymbol{\Xi} \boldsymbol{\Xi}^T] \mathbf{K}_{tt:i}^{1/2} \quad (99)$$

$$= \mathbf{K}_{ti} \mathbf{K}_{ii}^{-1} \mathbf{G}_{ii} \mathbf{K}_{ii}^{-1} \mathbf{K}_{ti}^T + \mathbf{K}_{tt:i} \quad (100)$$

For the full prediction algorithm, see Alg. 2.

F Fast solver for the input scale

At the first layer, we may use a linear kernel,

$$\mathbf{G}_1 = \mathcal{W} \left(\frac{1}{\nu} \mathbf{G}_0, \nu \right). \quad (101)$$

Remembering that $\mathbf{G}_0 = \frac{1}{\nu_0} \mathbf{X} \mathbf{X}^T$, is singular for large P , as it has rank $\min(\nu_0, P)$, this implies \mathbf{G}_1 , which has the same rank, may also be singular for large P . And in the case of singular \mathbf{G}_1 , our usual choice of objective breaks down. Instead, we consider scaling the input features using the Wishart-distributed matrix, $\boldsymbol{\Omega}$,

$$\boldsymbol{\Omega} \sim \mathcal{W} \left(\frac{1}{\nu_1} \mathbf{I}, \nu_1 \right) \quad \mathbf{G}_1 = \frac{1}{\nu_0} \mathbf{X} \boldsymbol{\Omega} \mathbf{X}^T \quad (102)$$

This choice allows us to scale the input features, without having to consider a singular scale matrix, as in Eq. (101). The terms in the objective that depend on $\boldsymbol{\Omega}$ are,

$$\mathcal{L}_M = T_1 + D'_2 + T_2 \quad (103)$$

$$T_1 = \frac{\nu_1}{2} \text{Tr}(\boldsymbol{\Omega}) \quad (104)$$

$$D'_2 = \frac{\nu_1}{2} \log |\boldsymbol{\Omega}| - \frac{\nu_2}{2} \log |\mathbf{K}(\mathbf{G}_1)| \quad (105)$$

$$T_2 = -\frac{\nu_2}{2} \text{Tr}(\mathbf{K}(\mathbf{G}_1)^{-1} \mathbf{G}_2), \quad (106)$$

Now, we define \mathbf{A}_ℓ , \mathbf{U}_ℓ and \mathbf{Q}_ℓ using gradients wrt $\mathbf{\Omega}$,

$$\mathbf{A}_1 = \frac{1}{2} \left. \frac{\partial D'_2}{\partial \mathbf{\Omega}} \right|_{\tilde{\mathbf{\Omega}}} \tilde{\mathbf{\Omega}} \quad (107a)$$

$$\mathbf{U}_1 = - \left. \frac{\partial T_1}{\partial \mathbf{\Omega}} \right|_{\tilde{\mathbf{\Omega}}} \quad (107b)$$

$$\mathbf{Q}_1 = \tilde{\mathbf{\Omega}} \left. \frac{\partial T_2}{\partial \mathbf{\Omega}} \right|_{\tilde{\mathbf{\Omega}}} \tilde{\mathbf{\Omega}} \quad (107c)$$

And we update $\mathbf{\Omega}$ by solving the CARE,

$$\mathbf{0} = \mathbf{A}_1^T \mathbf{\Omega} + \mathbf{\Omega} \mathbf{A}_1 - \mathbf{\Omega} \mathbf{U}_1 \mathbf{\Omega} + \mathbf{Q}_1. \quad (108)$$